Organic LETTERS

Letter

pubs.acs.org/OrgLett

K-Conjugated Dibenzoazahexacenes

Gabriella Antonicelli,[†] Cristian Gozalvez,[†] Ainhoa Atxabal,[‡] Manuel Melle-Franco,*[,§] Luis E. Hueso,*[,‡,∥] and Aurelio Mateo-Alonso*[,†,∥]

[†]POLYMAT, University of the Basque Country UPV/EHU, Avenida de Tolosa 72, E-20018 Donostia-San Sebastián, Spain

[‡]CIC Nanogune, Avenida de Tolosa 76, E-20018 Donostia-San Sebastián, Spain

[§]CICECO - Aveiro Institute of Materials, Department of Chemistry, University of Aveiro, 3810-193 Aveiro, Portugal

[∥]Ikerbasque, Basque Foundation for Science, Bilbao, Spain

Supporting Information

ABSTRACT: The synthesis and properties of two highly stable K-conjugated dibenzoazahexacenes are reported. Single-crystal X-ray, optoelectronic, and electrochemical characterization combined with theoretical studies show a favorable molecular packing and an optimal energy alignment of their frontier orbitals for charge transport. Electrical characterization illustrates that the preferential transport of holes or electrons depends on the number of N atoms in the aromatic framework.

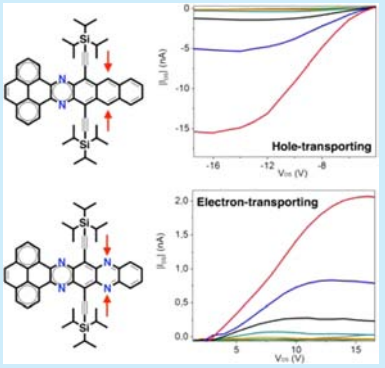

Nitrogenated polycyclic aromatic hydrocarbons (N-PAHs) are receiving a great deal of attention as a platform to design and synthesize organic semiconductors for a wide variety of applications.[1] In the acene series, it has been both predicted and demonstrated that the exchange of C atoms for N atoms in the aromatic framework provides to these otherwise hole-transporting materials the ability to transport electrons resulting in ambipolar or purely electron-transporting materials.[1h,i] Whereas charge transport in azaacenes with different numbers of N atoms and in different positions has been the subject of systematic investigations, few studies have focused so far on other N-PAHs. Among these, pyrene-fused azaacenes (PPA)[1a,2] are receiving great interest as precursors of narrow nanoribbon-like structures for organic electronic applications because of their enhanced length/stability relationship. In this paper, we report the synthesis and properties of K-conjugated dibenzoazahexacenes **1** and **2** (Scheme 1). Single-crystal X-ray, optoelectronic, and electrochemical characterization studies show a favorable molecular packing and an optimal energy alignment of their frontier orbitals for charge transport. Indeed, electrical characterization of field-effect transistors without any device optimization illustrate that dibenzoazahexacenes **1** and **2** behave as semiconductors. Furthermore, the preferential transport of holes or electrons depends on the number of N atoms in the aromatic framework. For instance, p-type transport has been observed for hexacene **1** with two N atoms embedded in the aromatic framework, while n-type transport has been observed for hexacene **2** with four N atoms, illustrating the multiple possibilities for modulating the properties of this family of N-PAHs.

Scheme 1. Synthetic Route for Dibenzoazahexacenes 1 and 2

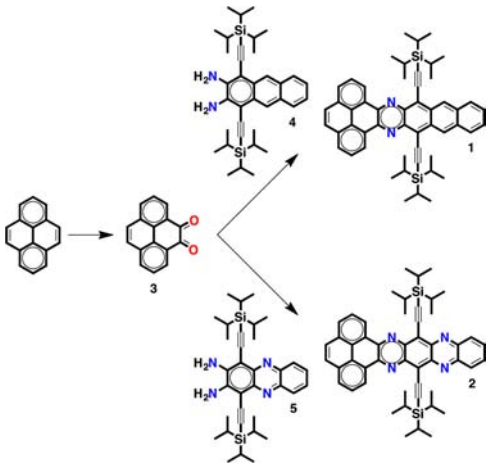

Dibenzoazahexacenes **1** and **2** were synthesized following the route depicted on Scheme 1. Full procedures are given in the Supporting Information (SI). Pyrene diketone **3** was synthesized in one step from pyrene following the procedure of Harris.[3] The corresponding diamines **4**[4] and **5**[5] were synthesized respectively from commercially available compounds following reported methods. Cyclocondensation of pyrene diketone **3** with diamines **4** and **5** in $CHCl_3$/AcOH (1:1)

Received: August 5, 2016
Published: September 7, 2016

DOI: 10.1021/acs.orglett.6b02332
Org. Lett. 2016, 18, 4694−4697

yielded respectively **1** and **2** in moderate yields (37% and 51%, respectively) as purple compounds. Compounds **1** and **2** are soluble in chlorinated solvents, including CH_2Cl_2, $CHCl_3$, and *o*-dichlorobenzene (ODCB).

Crystals suitable for X-ray diffraction were obtained by slow evaporation of solutions of **1** and **2** in $CHCl_3$, respectively (Figure 1). X-ray analysis not only confirms the structure but

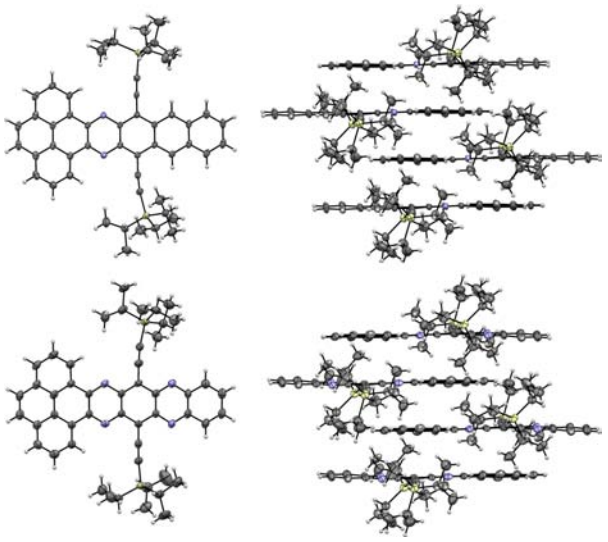

Figure 1. X-ray structures and packing of dibenzoazahexacenes **1** (top) and **2** (bottom).

also provides information about packing in the solid state. Remarkably, the difference in the number of N atoms in the aromatic core have an almost negligible effect on the overall structure besides the expected differences imposed by the different C═C and C═N distances. In both cases, the aromatic core of **1** and **2** is essentially flat while the pending ethynyl groups are out of plane because of the close proximity of the TIPS substituents to the protons located in positions 1, 2, 7, and 8 of the pyrene unit. Molecules of **1** and **2** pile-up in a similar antiparallel fashion so that bulky TIPS groups allow a face-to-face packing at 3.397 and 3.233 Å, respectively. The existing tight face-to-face packing provides a pathway for charge transport and suggests that both **1** and **2** can behave as semiconductors.

The electronic absorption spectra of **1** and **2** were recorded from ODCB solutions (Figure 2). The spectrum of hexacene **1**

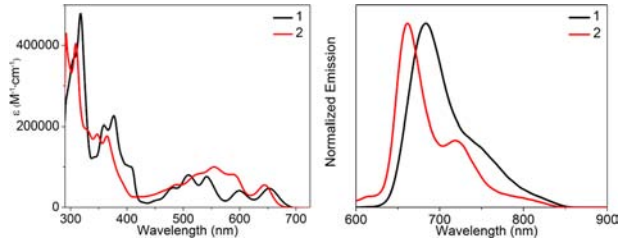

Figure 2. Absorption electronic (top) and photoluminescence (bottom) spectra of **1** and **2** in ODCB.

shows two sets of bands in the visible region with clear vibronic features that were assigned to the *ß* and *p* bands[6] respectively from lower to higher wavelengths, in analogy to acene derivatives. The longest-wavelength absorption of **1** (λ_{max}) appears at 652 nm. The spectrum of hexacene **2** (λ_{max} = 645 nm) does not differ much from that of **1**, which shows the same *ß* and *p* band structure but with evident energy shifts. For instance, the *ß* and *p* bands of hexacene **2** are clearly shifted toward lower and higher energies, respectively, when compared with **1**. These differences between **1** and **2** can be attributed to the presence of the two additional N atoms in **2** and are consistent with the larger change observed on the *ß* bands.[6] The photoluminescence spectra of **1** and **2** show an emission band with a vibronic structure that spans from the red into the near-infrared with maxima at 683 and at 661 nm, respectively.

We computed the first 12 singlet excitations with time-dependent density functional theory in ODCB with BMK and B3LYP Hamiltonians with a 6311+g(2d,p) basis set on B3LYP-odbc-6-31(d,p) minimized geometries (full details in SI). The two highest possible transitions are allowed and intense and correspond to the HOMO → LUMO and HOMO−1 → LUMO. The HOMO → LUMO wavelength for **1** and **2** with the BMK Hamiltonian are at 657 and 625 nm respectively which correlate very well with the experimental values (652 and 645 nm), as previously observed in a similar system.[2b]

Cyclic voltammetry studies were carried out in order to investigate the most accessible redox states (Figure 3). The cyclic

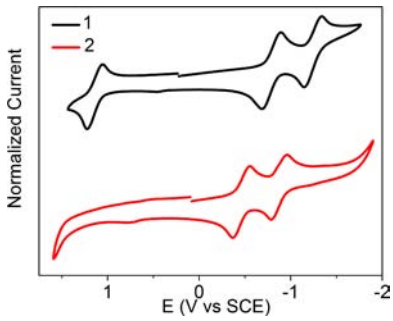

Figure 3. Cyclic voltammograms of **1** and **2** in 0.1 M nBu$_4$NPF$_6$ in ODCB.

voltammograms of **1** evidence two consecutive reversible reduction processes ($E_{1/2}$ = −0.81 and −1.26 V vs SCE) and one reversible oxidation process ($E_{1/2}$ = +1.18 V vs SCE) consistent with the electrogeneration of the radical anion, the dianion, and the radical cation, respectively, in analogy to phenazine derivatives.[7] The same reduction pattern was observed on the cyclic voltammograms of **2**, namely, two consecutive reversible reduction waves ($E_{1/2}$ = −0.52 and −0.94 V vs SCE). However, no sign of the reversible oxidation process was observed. The small residual current on the oxidation scan was attributed to some decomposition of the compound or of the solvent-supported electrolyte during the scans, as a scan on the corresponding potential window showed no measurable current (Figure S9).

The optical HOMO−LUMO gaps (E_{gap}^{opt}) of **1** and **2** were estimated from the longest-wavelength absorption and correspond to 1.81 and 1.85 eV, respectively. The electrochemical LUMO levels or electron affinities (E_{LUMO}) were estimated from the potential onsets of the first reduction waves. The E_{LUMO} for **1** and **2** correspond to −3.57 and −3.89 eV, respectively. The E_{LUMO} of **2** is 0.3 eV lower than that of **1**, which is consistent with the two additional N atoms embedded in the aromatic framework. The reversible oxidation redox process for hexacene **1** allows estimating the electrochemical

DOI: 10.1021/acs.orglett.6b02332
Org. Lett. 2016, 18, 4694−4697

HOMO level (E_{HOMO}^{CV} = −5.43 eV) from the onset of the oxidation wave and the electrochemical HOMO−LUMO gap (E_{gap}^{CV} = 1.85 eV), which is in agreement with that estimated optically. Similar trends were observed on the energy levels for **1** and **2** estimated theoretically at B3LYP/6-311+g(2d,p) and at BMK/6-311+g(2d,p) (full details in the SI). Eigenvalues for B3LYP give a good estimate of the E_{LUMO} (−3.31 and −3.36 eV) and of the gaps (2.00 and 2.06 eV) in ODCB and vacuum, as previously noted.[2b] In all other cases BMK provides better estimates.

As mentioned above **1** and **2** show a similar electronic structure to acenes. Remarkably, the E_{gap}^{opt} values of **1** (1.81 eV) and **2** (1.85 eV) are similar to those of TIPS-pentacene (1.83 eV),[1f,g,8] TIPS-tetraazapentacene (1.82 eV),[9] and a substantially longer dibenzooctaazadecacene (1.86 eV).[10] This implies that the sextets in the lateral rings contribute to the linear conjugation and provide dibenzoazahexacenes **1** and **2** with an acene character similar to pentacene. This is consistent with calculations carried out at the BMK-odbc-6311+g(2d,p)/B3LYP-odbc-6-31(d,p) level that show similar electron densities in the frontier orbitals of **1** and **2** compared to TIPS-pentacene[1f,g,8] and TIPS-tetraazapentacene[9] (Figure 4).

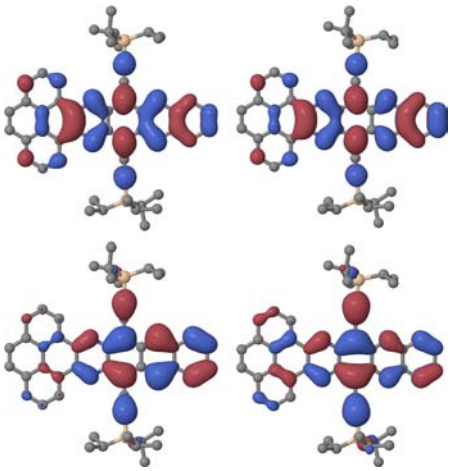

Figure 4. HOMO (bottom) and LUMO (top) of **1** (left) and **2** (right).

To shine light on the charge transport properties of **1** and **2** a series thin-film field-effect transistors were fabricated and studied without any device optimization. Thermal gravimetric analysis of **1** and **2** reveals that both compounds are very stable even at high temperatures and therefore that they can be deposited by sublimation. In fact no sign of decomposition was observed under nitrogen until 388.5 and 381.1 °C for **1** and **2**, respectively (Figure S8). Compounds **1** and **2** were independently vacuum-deposited on bottom-contact bottom-gate transistors fabricated on Si/SiO_2 substrates on top of which gold source and drain electrodes had been evaporated. Before the deposition of the semiconducting layer, the SiO_2 surface had been previously modified with octadecyltrichlorosilane (OTS). Full details on the structure and characterization of the devices are given in the Supporting Information. The films of **1** show the typical behavior for p-type semiconductors, and hole mobilities (μ_h) of 4.30 × 10^{-4} cm^2 V^{-1} s^{-1} were observed for the best performing transistor (average μ_h = 2.15 × 10^{-4} cm^2 V^{-1} s^{-1}) with moderate on/off currents ($I_{on/off}$) in the range of 10^1 (Figure 5 top). Remarkably the thin films of compound **2**

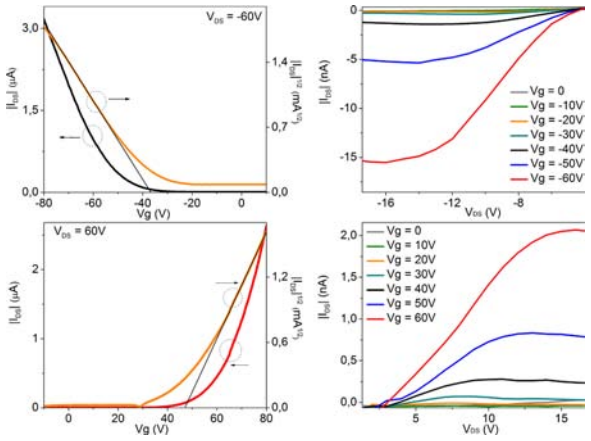

Figure 5. Representative transfer and square root of the absolute values of current as a function of gate potential (left), and output (right) curves of thin films dibenzoazahexacenes **1** (top) and **2** (bottom).

that present two additional N atoms in the aromatic framework show the typical behavior for n-type semiconductors and electron mobilities (μ_e) of 6.04 × 10^{-4} cm^2 V^{-1} s^{-1} were observed for the best performing transistor (average μ_e = 1.57 × 10^{-4} cm^2 V^{-1} s^{-1}) with $I_{on/off}$ in the range of 10^2 (Figure 5 bottom). Depositing the semiconductors at higher substrate temperatures or annealing of the devices deposited at room temperature result in lower charge carrier mobilities. The morphology of the films was investigated by atomic force microscopy that confirmed a substantial change of morphology with increasing temperatures that was linked to the lower performance (Figures S9 and S10).

The transport of different types of charge carriers in the thin films of **1** and **2** can be rationalized in terms of the intrinsic stabilization of the HOMO and LUMO with the number of N atoms present in the aromatic framework. In the case of **1**, the HOMO aligns better with the Fermi level of the gold electrodes favoring the injection of holes. On the other hand, in the case of **2**, the two additional N atoms stabilize both frontier orbitals, so the LUMO aligns at a larger extent with the Fermi energy of gold favoring the injection of electrons.

We have described the synthesis of two K-conjugated dibenzoazahexacenes that are remarkably stable (up to ∼380 °C under nitrogen). Even if dibenzoazahexacenes **1** and **2** vary in the number of N atoms in the aromatic framework (two and four, respectively), they pack in a similar π−π face-to-face fashion in the solid state at virtually the same distance as the graphite interlayer distance, as observed by X-ray crystallography. Their optoelectronic properties, estimated by optical and electrochemical measurements, reveal HOMO−LUMO gaps similar to TIPS-pentacene[8] and TIPS-tetraazapentacene.[9] Charge transport studies carried out on vacuum-deposited thin films show p-type transport for **1** and n-type transport for **2** with similar mobilities in the range of 10^{-4} cm^2 V^{-1} s^{-1} without any device optimization. These differences can be rationalized in terms of the energy of their HOMO and LUMO levels of **1** and **2** that correlate directly with the number of N atoms.

■ ASSOCIATED CONTENT

Supporting Information

The Supporting Information is available free of charge on the ACS Publications website at DOI: 10.1021/acs.orglett.6b02332.

DOI: 10.1021/acs.orglett.6b02332
Org. Lett. 2016, 18, 4694−4697

Synthesis and characterization of **1** and **2** (PDF)
Crystallographic data for **1** (CIF)
Crystallographic data for **2** (CIF)

AUTHOR INFORMATION

Corresponding Authors

*E-mail: amateo@polymat.eu (A.M.-A.).
*E-mail: manuelmelle.research@gmail.com (M.M.-F.).
*E-mail: l.hueso@nanogune.eu (L.E.H.).

Notes

The authors declare no competing financial interest.

ACKNOWLEDGMENTS

We are grateful to the Basque Science Foundation for Science (Ikerbasque), POLYMAT, the University of the Basque Country (SGIker), Deutsche Forschungsgemeinschaft (AU 373/3-1 and MA 5215/4-1), Gobierno de España (Ministerio de Economía y Competitividad, MAT2012-35826 and MAT2015-65159-R), Gobierno Vasco (BERC program and PC2015-1-01(06-37)), Diputación Foral de Guipuzkoa (2015-CIEN-000054-01), CICECO - Aveiro Institute of Materials, POCI-01-0145-FEDER-007679 (FCT ref. UID/CTM/50011/2013), ON2 (NORTE-07-0162-FEDER-000086), and the European Union (ERA-Chemistry, Career Integration Grant No. 618247, and FEDER). This project has received funding from the *European Union's Horizon 2020 research and innovation programme* under grant agreement No. 664878.

DEDICATION

Dedicated to Professor Nazario Martín on the occasion of his 60th birthday.

REFERENCES

(1) (a) Mateo-Alonso, A. *Chem. Soc. Rev.* **2014**, *43*, 6311. (b) Bunz, U. H. F. *Acc. Chem. Res.* **2015**, *48*, 1676. (c) Bunz, U. H. F.; Engelhart, J. U.; Lindner, B. D.; Schaffroth, M. *Angew. Chem., Int. Ed.* **2013**, *52*, 3810. (d) Bunz, U. H. F. *Pure Appl. Chem.* **2010**, *82*, 953. (e) Bunz, U. H. F. *Chem. - Eur. J.* **2009**, *15*, 6780. (f) Anthony, J. E. *Angew. Chem., Int. Ed.* **2008**, *47*, 452. (g) Anthony, J. E. *Chem. Rev.* **2006**, *106*, 5028. (h) Miao, Q. *Adv. Mater.* **2014**, *26*, 5541. (i) Winkler, M.; Houk, K. N. *J. Am. Chem. Soc.* **2007**, *129*, 1805. (j) Stępień, M.; Gońka, E.; Żyła, M.; Sprutta, N. *Chem. Rev.* **2016**, DOI: 10.1021/acs.chemrev.6b00076.

(2) (a) Jiang, L.; Papageorgiou, A. C.; Oh, S. C.; Sağlam, Ö.; Reichert, J.; Duncan, D. A.; Zhang, Y.-Q.; Klappenberger, F.; Guo, Y.; Allegretti, F.; More, S.; Bhosale, R.; Mateo-Alonso, A.; Barth, J. V. *ACS Nano* **2016**, *10*, 1033. (b) Marco, A. B.; Gozalvez, C.; Olano, M.; Sun, X.; Atxabal, A.; Melle-Franco, M.; Hueso, L. E.; Mateo-Alonso, A. *Phys. Chem. Chem. Phys.* **2016**, *18*, 11616. (c) Marco, A. B.; Cortizo-Lacalle, D.; Gozalvez, C.; Olano, M.; Atxabal, A.; Sun, X.; Melle-Franco, M.; Hueso, L. E.; Mateo-Alonso, A. *Chem. Commun.* **2015**, *51*, 10754. (d) Garcia, R.; Melle-Franco, M.; Mateo-Alonso, A. *Chem. Commun.* **2015**, *51*, 8037. (e) More, S.; Choudhary, S.; Higelin, A.; Krossing, I.; Melle-Franco, M.; Mateo-Alonso, A. *Chem. Commun.* **2014**, *50*, 1976. (f) More, S.; Bhosale, R.; Mateo-Alonso, A. *Chem. - Eur. J.* **2014**, *20*, 10626. (g) García, R.; More, S.; Melle-Franco, M.; Mateo-Alonso, A. *Org. Lett.* **2014**, *16*, 6096. (h) More, S.; Bhosale, R.; Choudhary, S.; Mateo-Alonso, A. *Org. Lett.* **2012**, *14*, 4170. (i) Kulisic, N.; More, S.; Mateo-Alonso, A. *Chem. Commun.* **2011**, *47*, 514. (j) Mateo-Alonso, A.; Kulisic, N.; Valenti, G.; Marcaccio, M.; Paolucci, F.; Prato, M. *Chem. - Asian J.* **2010**, *5*, 482. (k) Mateo-Alonso, A.; Ehli, C.; Chen, K. H.; Guldi, D. M.; Prato, M. *J. Phys. Chem. A* **2007**, *111*, 12669.

(3) Hu, J.; Zhang, D.; Harris, F. W. *J. Org. Chem.* **2005**, *70*, 707.

(4) (a) Appleton, A. L.; Miao, S.; Brombosz, S. M.; Berger, N. J.; Barlow, S.; Marder, S. R.; Lawrence, B. M.; Hardcastle, K. I.; Bunz, U. H. F. *Org. Lett.* **2009**, *11*, 5222. (b) Appleton, A. L.; Brombosz, S. M.; Barlow, S.; Sears, J. S.; Bredas, J.-L.; Marder, S. R.; Bunz, U. H. F. *Nat. Commun.* **2010**, *1*, 91.

(5) Lindner, B. D.; Engelhart, J. U.; Tverskoy, O.; Appleton, A. L.; Rominger, F.; Peters, A.; Himmel, H.-J.; Bunz, U. H. F. *Angew. Chem., Int. Ed.* **2011**, *50*, 8588.

(6) (a) Clar, E. *The Aromatic Sextet*; Wiley: London, 1972. (b) Clar, E.; Guye-Vuillème, J. F.; McCallum, S.; Macpherson, I. A. *Tetrahedron* **1963**, *19*, 2185.

(7) (a) Alonso, A. M.; Horcajada, R.; Motevalli, M.; Utley, J. H. P.; Wyatt, P. B. *Org. Biomol. Chem.* **2005**, *3*, 2842. (b) Alonso, A. M.; Horcajada, R.; Groombridge, H. J.; Chudasama, R.; Motevalli, M.; Utley, J. H. P.; Wyatt, P. B. *Org. Biomol. Chem.* **2005**, *3*, 2832. (c) Alonso, A. M.; Horcajada, R.; Groombridge, H. J.; Mandalia, R.; Motevalli, M.; Utley, J. H. P.; Wyatt, P. B. *Chem. Commun.* **2004**, 412.

(8) Griffith, O. L.; Anthony, J. E.; Jones, A. G.; Shu, Y.; Lichtenberger, D. L. *J. Am. Chem. Soc.* **2012**, *134*, 14185.

(9) Miao, S.; Appleton, A. L.; Berger, N.; Barlow, S.; Marder, S. R.; Hardcastle, K. I.; Bunz, U. H. F. *Chem. - Eur. J.* **2009**, *15*, 4990.

(10) Wang, Z.; Miao, J.; Long, G.; Gu, P.; Li, J.; Aratani, N.; Yamada, H.; Liu, B.; Zhang, Q. *Chem. - Asian J.* **2016**, *11*, 482.

DOI: 10.1021/acs.orglett.6b02332
Org. Lett. 2016, 18, 4694−4697